Time-Of-Flight Spectrometry and Performance of a Pulsed Plasma Thruster with Non-Volatile Propellant

IEPC-2015-141／ISTS-2015-b-141

Presented at Joint Conference of 30th International Symposium on Space Technology and Science, 34th International Electric Propulsion Conference and 6th Nano-satellite Symposium
Hyogo-Kobe, Japan
July 4–10, 2015

S. Barral[1]
QuinteScience, 00429 Warsaw, Poland

J. Kurzyna[2], A. Szelecka[3], H. Rachubiński[4], D. Daniłko[5]
Institute of Plasma Physics and Laser Microfusion, 01497 Warsaw, Poland

R. Martín[6], E. Remírez[7]
JMP Ingenieros, 26371 Sotés (la Rioja), Spain

P. Ortiz[8], J. Alonso[9]
Najera Aerospace, 26371 Sotés (la Rioja), Spain

Y. Mabillard[10], S. Bottinelli[11]
Mecartex, 6933 Muzzano, Switzerland

A. Zaldívar[12], P. Rangsten[13]
NanoSpace AB, Uppsala Science Park, SE-751 83 Uppsala, Sweden
and
C. R. Koppel[14]
KopooS Consulting Ind., 75008 Paris, France

Abstract: The performance of the second design iteration of a PPT operating with non-volatile propellant is reported, consolidating the encouraging results obtained earlier with a proof-of-concept design. In particular, an efficiency of the order of 10% has been maintained at all tested operating points for Isp ranging from 900 to 1400 s, despite small thruster size and moderate pulse energy (~1J). Time-of-flight measurements have been also performed with a retarded potential analysis to derive the mass-energy spectrum of ions in the far plume, which suggests an unexpectedly large contribution of multiply charged C and F ions. Finally, fast camera imaging has been used in correlation with current measurements in an attempt to qualitatively capture the time evolution of the discharge topology..

[1]Chief engineer, serge.barral@quintescience.com.
[2]Research associate, Division of Magnetized Plasmas, jacek.kurzyna@ipplm.pl.
[3]Research assistant, Division of Magnetized Plasmas, agnieszka.szelecka@ipplm.pl.
[4]Research assistant, Division of Magnetized Plasmas, hubert.rachubinski@ipplm.pl.
[5]Research assistant, Division of Magnetized Plasmas, dariusz.danilko@ipplm.pl.
[6]Project manager, ricardo.martin@jmpingenieros.es.
[7]Chief executive officer, eduardo.remirez@jmpingenieros.es.
[8]Electronic system design engineer, pablo.ortiz@nasp.es.
[9]Electronic system design engineer, javier.alonso@nasp.es.
[10]Head of R&D, yann.mabillard@mecartex.ch.
[11]Chief executive officer, stefano.bottinelli@mecartex.ch.
[12]Development engineer, ana.salaverri@sscspace.com.
[13]Vice president engineering, pelle.rangsten@sscspace.com.
[14]Chief consulting engineer, christophe.koppel@kopoos.com.

Nomenclature

C_0	effective capacitance
E	discharge energy
I_{bit}	impulse bit
I_{sp}	specific impulse
L	distance between thruster and RPA
m	ion mass
P	tank pressure
ΔP	pressure gradient in the restriction
q	ion charge
Q_v	propellant volumetric flow rate
T	temperature of the restriction
v	ion velocity
V_0	capacitor threshold voltage
V_{G2}	retarding potential
$\mathcal{V}$	dispensing volume
η	thruster efficiency
μ	dynamic viscosity of propellant
τ_{on}	valve opening time

I. Introduction

The simplicity and scalability of Pulsed Plasma Thrusters (PPTs) makes them ideal for the propulsion of nano-satellites, as witnessed by the strong resurgence of interest for this plasma propulsion device. The maturity of the conventional Teflon propellant PPT, which has existed for more than 50 years, certainly contributes to the appeal of this technology. The adoption of a solid propellant comes, however, with a number of limitations such as the lack of propellant feed rate control, the impossibility to use common propellant storage in multi-thruster configurations, and variation of impulse bit throughout lifetime.

The L-µPPT project attempts to remedy those issues with the development of a novel PPT concept based on a liquid propellant. Unlike former attempts at operating a PPT with a liquid propellant,[1–10] however, a non-volatile fluoro-polymer fluid was selected that circumvents the many issues associated with the dispensing of a volatile liquid in vacuum. By using an open-slit dispensing design, the simplicity of ablative PPTs is combined with the advantages inherent to liquid propellants. This feeding method also allows a reduction of the exposed propellant surface, which is theorized to mitigate late-time ablation propellant losses. The chosen propellant has in turn many advantages over other liquid propellants in common use: it is non-toxic, chemically stable, remains in a liquid state from -50°C to 150°C, is much denser than water, does not require pressurization and is space-qualified as a lubricant.

The present work reports performance characterizations for a second generation L-µPPT designed based on the lessons learned with the initial prototype.[11,12] This second design allowed the mass flow rate to be precisely characterized, leading to the first complete assessment of the thruster performance including specific impulse. As a part of a long-haul effort to understand the physics at play and identify the parameters that most affect thruster performance, a Time-Of-Flight (TOF) characterization of the plume was also performed and complemented by fast camera imaging of the discharge.

II. Thruster design

A. General design

Due to the apparent absence of charring on the propellant surface and the very encouraging performance level of the first thruster prototype, the same PFPE fluid has been selected to operate the second prototype. The main reasons that motivated the choice of PFPE in the first place have been enumerated earlier[11,12] and include non-hazardousness, hydrophobicity, high density, very high chemical stability, extreme liquid

phase temperature range, qualification for space use, space optics compatibility and negligible outgassing.

The first prototype was initially meant to operate with a syringe micropump feeding the propellant through an orifice. It was rapidly realized,[12] however, that proper thruster operation required the existence of a film of propellant between the anode and cathode to forms a precursor path for the flashover discharge. For this reason, the second prototype delivers the propellant into a slit that extends between the main electrodes. In order to limit the influence of gravity on the shape of the free liquid surface, the slit is placed horizontally with the electrodes located on either side of the thruster body. Undesired propellant migration within interstitial spaces (*creeping*) is avoided by means of capillary traps near each electrode (Fig. 1).

B. Nominal propellant dispensing method

The nominal propellant dispensing method for the second prototype is based on time-metered flow rate control with a simple solenoid valve and a capillary restriction. The advantages of the time-metering method are its simplicity and the possibility to manage large volumes of stored propellant, which was not possible with the former syringe pump. Its principle leverages the fact that, unlike other liquid propellant electric thrusters such as colloid thruster, the L-µPPT does not require continuous propellant feeding. In fact, the only requirement is to keep at any time enough propellant in the open slit to ensure that it is fully wet, which can be achieved using periodic propellant delivery with dispensed volumes in the milliliter range. This is a drastic simplification compared *e.g.* to colloid thrusters where complex and heavy proportional valves are required for direct flow rate control.

Time-metering for viscous flows relies on the application of Poiseuille's law across a calibrated restriction:

$$Q_v = \frac{\pi d^4 \Delta P}{128 \mu L} \,, \tag{1}$$

which states that in a long capillary of diameter d, the mass flow rate is proportional to the pressure gradient ΔP and inversely proportional to the dynamic viscosity of the fluid μ. For the present case where the pressure at the orifice of the capillary is zero (vacuum conditions), it is sufficient to know the upstream pressure P to obtain the pressure differential. The viscosity is, in turn, a function of temperature T and can therefore be characterized by a measurement of the temperature at the restriction. Therefore, controlled amounts of propellant can be dispensed through a calibrated capillary by varying the valve's opening time as a function of the upstream pressure and of the temperature using the simple proportionality relation:

$$\tau_{on} \propto \frac{\mathcal{V} \mu\,(T)}{P} \tag{2}$$

where τ_{on} is the opening time and $\mathcal{V}$ is the targeted volume to be dispensed.

The electrical design remains similar to that of conventional PPTs, with a spark gap located close to the free surface of the propellant. The capacitor bank design inherits from the first prototype but has benefited from improvements with respect to manufacturing methods. Also, instead of using common intermediate electrodes between the two capacitors layers of each of the two sub-banks, each capacitor pair has an independent serial connection strip. Two type of capacitors have been used, both based on the same ceramic technology and with similar energy density but different nominal voltages.

The general conceptual design is shown in Fig. 2.

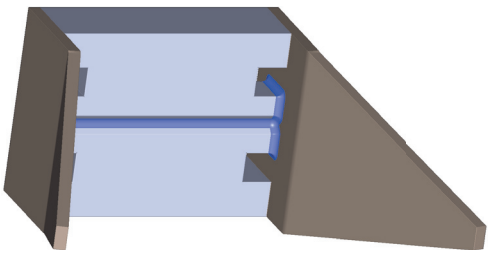

Figure 1. Illustration of the open slit propellant feeding principle (propellant meniscus shown in blue). Capillary traps are located near each electrode to prevent propellant migration via creeping in interstitial spaces.

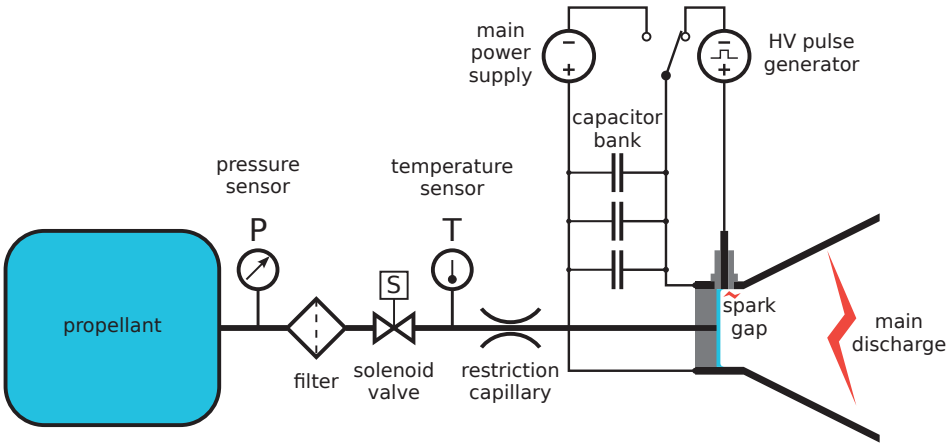

Figure 2. Schematic of the second L-µPPT prototype design.

C. Simplified feeding method for mass loss measurement

Although the time-metered feeding method was found to work reliably in a tightly controlled environment, due to the very short development time of the second prototype, the implementation of the feeding system was far from optimal and not robust enough for reliable operation in vacuum. In particular, the high filter hydraulic impedance and the high hydraulic compliance (capacitance) of the feed line made the flow rate very sensitive to the detailed routing of the feed line. Also, for lack of a dedicated setup to fill the tank, trapped air bubbles frequently interfered with propellant dispensing.

In order to perform a direct measurement of the mass loss, an alternative, simpler propellant feeding system was eventually adopted which consists in a ∅1 mm ID tube mounted at the back of the dispensing plate. This thin tube was used as a small tank able to hold more than 20 mg of propellant, which is typically enough for about 10000 discharges. Due to the slightly unfavorable balance of capillary forces between this tube and the dispensing groove, pure capillary feeding of the groove was not possible and it was necessary to add a small amount of hydrostatic pressure by pointing the thruster slightly downwards by some 5°.

D. Capacitance and stored energy

Two capacitor banks with similar nominal energy density but different nominal voltage have been used, referred to later as the low voltage and high voltage banks. The energy stored in the capacitor banks as a function of the voltage has been measured to enable thruster efficiency computations. Several methods for energy measurements have been employed, all leading to very similar estimates. Ultimately, a time-resolved voltage measurement of the bank discharge through a high power metal film resistor was chosen as the most reliable method, which by integration of the power V^2/R dissipated in the resistor provides the energy at all voltages down to zero in a single measurement. This measurement was repeated 3 times for each capacitor bank.

It was found that the experimental energy curves could be very closely fitted with the following analytical formula:

$$E(V) = \frac{1}{2} C_0 \frac{V^2}{1 + \frac{V}{V_0}} \tag{3}$$

where the ratio V/V_0 accounts for capacitance de-rating at high voltage. The fitting parameters for low and high voltage banks are, respectively:

$$\begin{aligned} C_0 &= 4.50\,\mu\text{F},\ V_0 = 1250\,\text{V} \\ C_0 &= 2.55\,\mu\text{F},\ V_0 = 1800\,\text{V} \end{aligned}$$

Although the large value of C_0 are at odds with the nominal (low voltage) capacitance provided by the manufacturer, these curves provide an excellent approximation above 100 V as can be judged from Fig. 3. The effective capacitance from the point of view of energy storage is actually higher than the nominal

capacitance up to about 30% of the nominal voltage; above this threshold, energy storage progressively worsens and becomes somewhat lower than the manufacturer non-derated values.

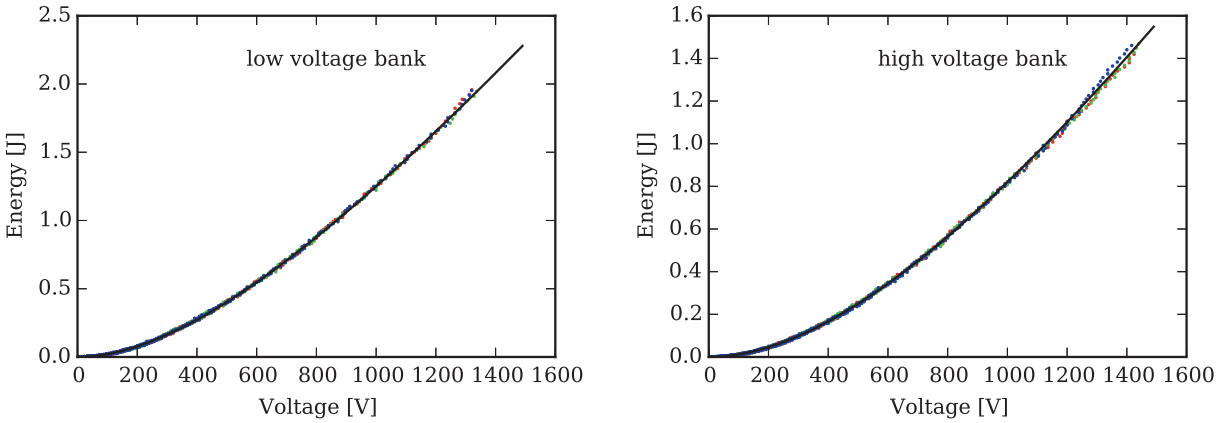

Figure 3. Experimentaly measured bank energy as a function of voltage (colored dots, 3 measurements) and analytical fit from Eq. (3) (black solid lines).

III. Performance characterization

A. Setup and measurement method

All measurement were performed in a vacuum chamber with volume approximately $2.2\,\mathrm{m}^3$ and diameter Ø1.2 m. A $3000\,\mathrm{l\,s}^{-1}$ (N_2) turbomolecular pump backed by a multistage roots pump of maximum speed $450\,\mathrm{m}^3\mathrm{h}^{-1}$ enabled continuous propellant pumping during thruster operation while maintaining the pressure under 10^{-5} mbar.

Unlike the traditional rotating arm design of impulse bit balances,[5,13–18] the balance designed at Mecartex uses a compact construction that relies on high precision flexure-based linear guiding and on a stiffness adjustment mechanism, allowing stiffness to be regulated over a very wide range down to zero. A non-contact voice-coil actuator was used to calibrate the thrust balance, which was done systematically after each measurement using a preset value of $20\,\mu$Ns. The moving mass of the thrust stand was ultimately inferred by averaging all such calibration impulses from all series made with the same load on the thrust stand. Knowing the moving mass, the amplitude and frequency of the thruster-generated balance oscillations were converted to impulse bit using an automated filtering and sine-matching algorithm described earlier.[12] The impulse bit was typically measured every 200 discharges in series of 10 consecutive measurements.

The mass bit was inferred from the mass loss of the front plate and attached capillary during a session, each session containing from 1400 to 2200 discharges. A high precision analytical balance with an error of ±0.1mg was used, hence an estimated mass bit measurement error per session below ±0.1 µg.

Further details about the setup and measurement procedure are available in earlier reports.[11,12]

B. Tests overview

The operating points that have been most thoroughly investigated and which are reported further are:

- 750 V operating voltage, low voltage bank ($E \approx 0.79\,\mathrm{J}$),
- 1000 V operating voltage, low voltage bank ($E \approx 1.25\,\mathrm{J}$),
- 1500 V operating voltage, high voltage bank ($E \approx 1.56\,\mathrm{J}$).

The visual appearance of the discharge is shown on Fig. 4. It is broadly similar to that seen with the first prototype,[12] but unlike the first prototype the discharge path clearly follows the propellant feeding groove.

No bank failure was observed during the preliminary tests and during the performance tests, with more than 30000 discharges accumulated on the low voltage bank, including about 20000 discharges at 750 V (many of which as part of initial testing and thus not included in the later analysis) and 10000 discharges at 1000 V.

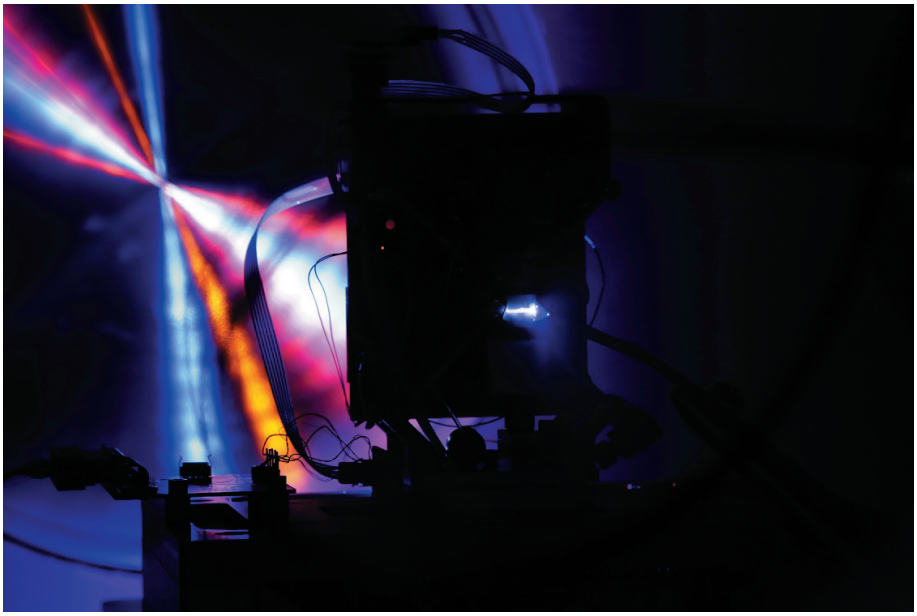

Figure 4. Long exposure photograph of the discharge at 750 V with the low voltage bank.

More than 2000 discharges were made with the high voltage bank operated at 1500 V, which was still properly operating at the end of the performance tests.

After the completion of performance testing, a lifetime testing of the low voltage bank was performed at 1000 V, which ended after 17633 discharges at 1000 V and a total of 47853 cumulated discharges after a capacitor failure. The reason for the capacitor failure is unknown, but it is possible that the bank had been excessively stressed at the beginning of its exploitation due to a faulty wiring that had exposed the bank to several thousands low power but high voltage (10 kV) pulses from the spark generator.

C. Performances at 750 V with the low voltage bank

The thrust history and performance at 750 V are shown on Fig 5, covering more than 10000 discharges and more than 500 thrust measurements. Although variations of performance were observed from session to session, these must be to a large extent attributed to statistical variations; session-averaged I_{sp} and efficiency remained relatively stable.

While the thrust-to-power ratio was about twice lower than in the first prototype,[12] this was presumably rather a consequence of operation at higher I_{sp} than the sign of a degradation of the thruster efficiency (note that efficiency could not be computed on the first prototype). Indeed, the efficiency shown on Fig. 5 — around 10% — is very high for a PPT, especially considering its small size, and it is unlikely that the first prototype would have operated at higher efficiency.

The thrust-to-power ratio remains relatively high, however, in comparison with the flight qualified LES-6 (14 µN/W[19]) and Dawgstar (10.7 µN/W[20]) thrusters and in line with the state-of-the-art PPTCUP thruster (16.5 µN/W[21] to 19 µN/W[22]), but with the advantage of a significantly higher I_{sp}.

It is believed that the main reason for the differences in terms of thrust-to-power ratio (and probably in terms I_{sp}) with the first prototype are attributable to the exposed area of propellant: whereas the first prototype had its whole front plate wetted by propellant (about 100 mm^2), in the second prototype only the propellant in the dispensing groove is exposed, which is about 10 mm^2. The tests at 1000 V discussed in section D provide further hindsights and support for this hypothesis.

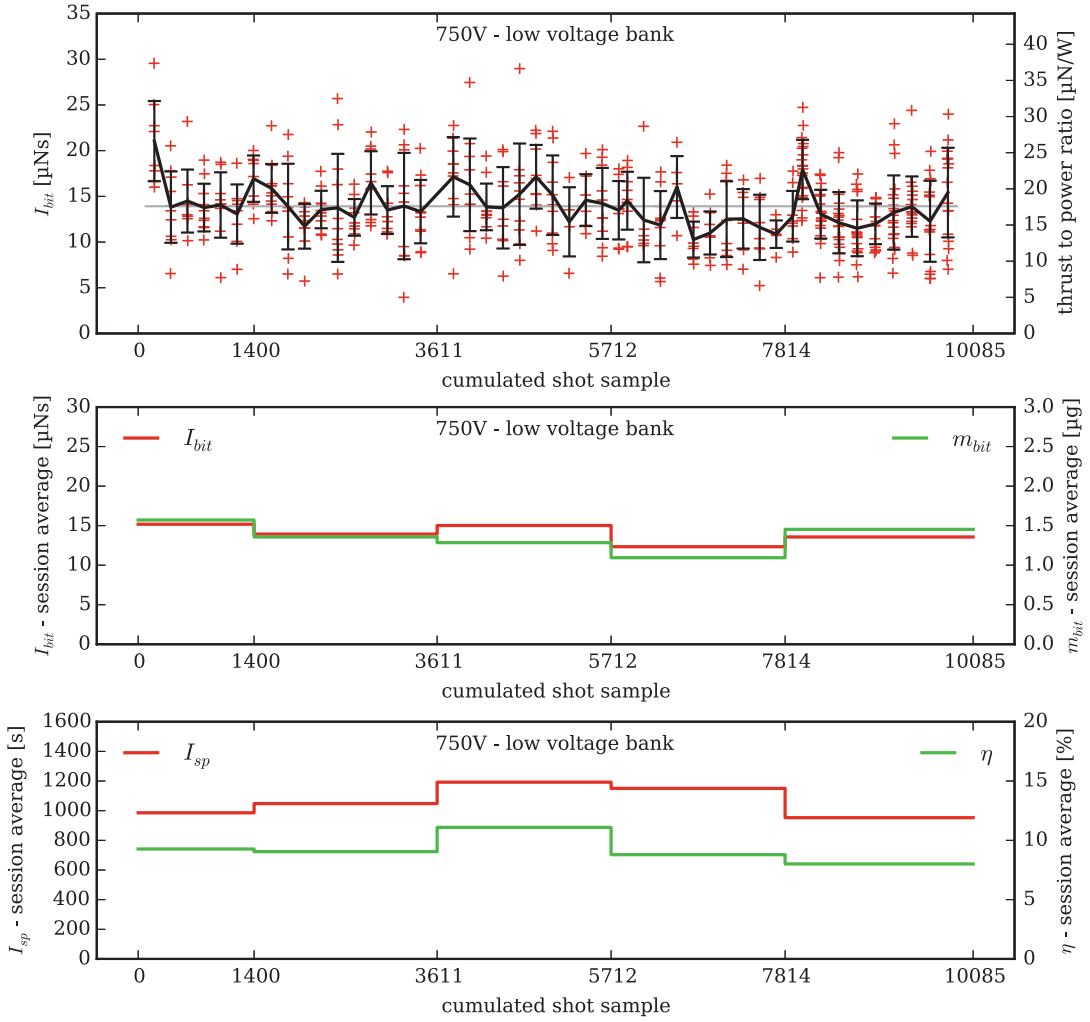

Figure 5. Thruster performance at 750 V with the low voltage bank for all experimental sessions.

D. Performances at 1000 V with the low voltage bank

The thrust history and calculated performance at 1000 V (Fig. 6) show a steady decrease during the first 2 sessions, which was already hinted at during the 2 last sessions at 750 V. This turned out to be related to the decreasing level of propellant in the miniature capillary tank and subsequent reduction of the exposed propellant area. Indeed, the tank had not been filled since the beginning of testing at 750 V and the level of propellant in the miniature tank was very low by the end of the second session at 1000 V. The groove was also visibly much less filled due to the lower hydrostatic pressure when the miniature tank is empty (see Fig. 7). Once refilled, the thrust-to-power ratio returned to values close to what was seen at 750 V.

Another element that strongly hints at the influence of the exposed propellant area is the peak of thrust in the middle of session 3 at 1000 V (see circled data on Fig. 6). Once the thruster was removed from the chamber at the end of the third session, even though there was no more propellant on the front plate (as it had presumably been ablated), traces of PFPE in location not exposed to the plasma made it clear that propellant leakage from the groove had occurred at some time during this session, probably due to over-filling of the miniature tank. It seems thus reasonable to attribute the temporary increase of thrust to the wetting of the front plate when the propellant leaked out of the groove.

Considering therefore only the 4th and 5th sessions (the mass bit measurement for the 3rd session was invalidated due to the leakage), the performances are in par with those at 750 V, showing a similar efficiency at 10%, a slightly higher I_{sp} and thus slightly lower thrust-to-power ratio.

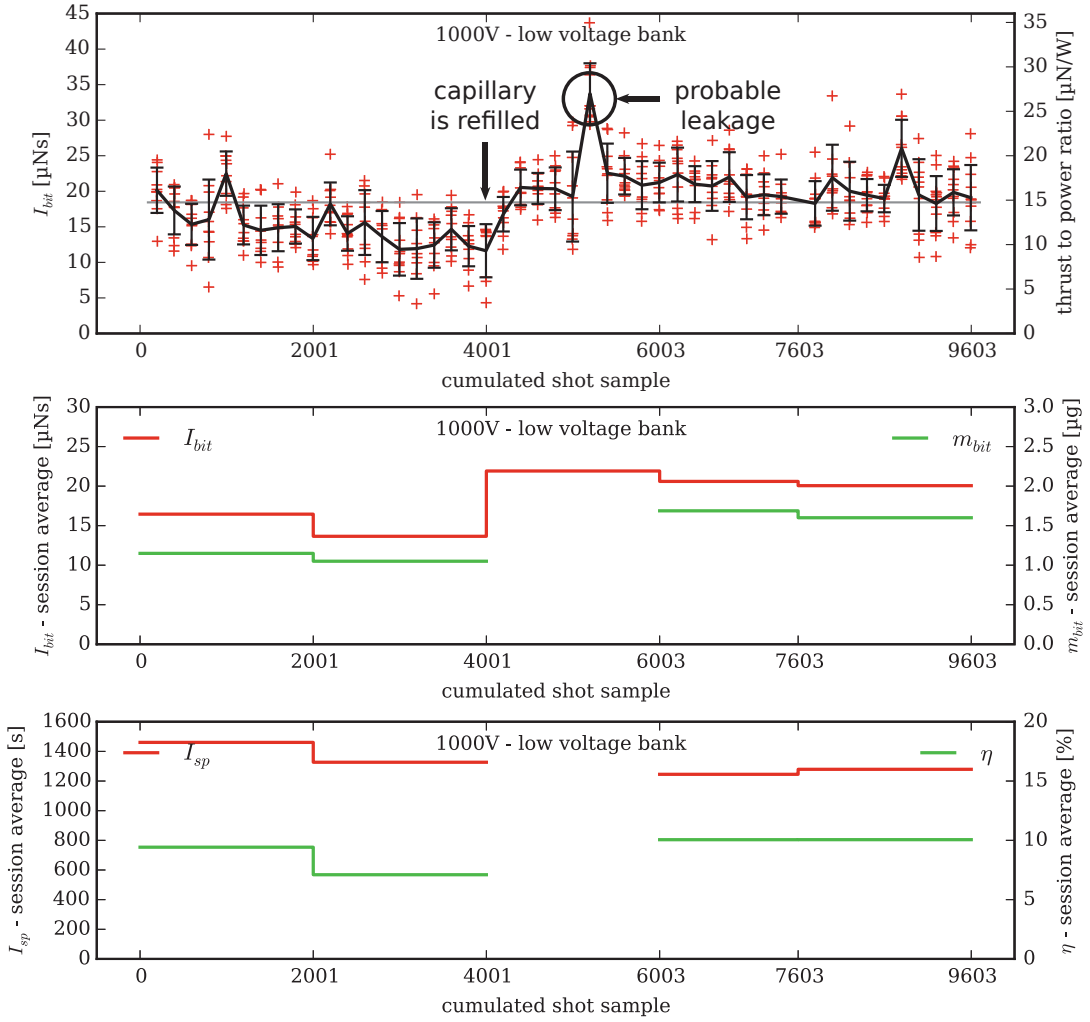

Figure 6. Thruster performance at 1000 V with the low voltage bank for all experimental sessions. Note that the mass bit measurement at session 3 was invalidated due to a small leakage of propellant down the front plate.

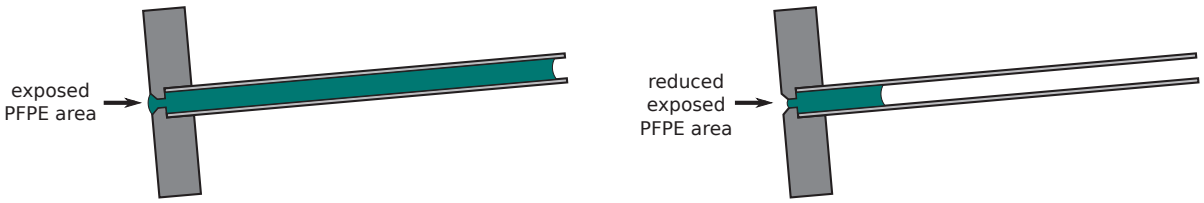

Figure 7. Influence of the quantity of propellant in the miniature capillary tank on the exposed area of propellant: as the level of propellant decreases, hydrostatic pressure becomes unable to overcome capillary forces that pull the propellant up in the capillary, thus preventing proper wetting of the groove (the groove direction is perpendicular to the drawing).

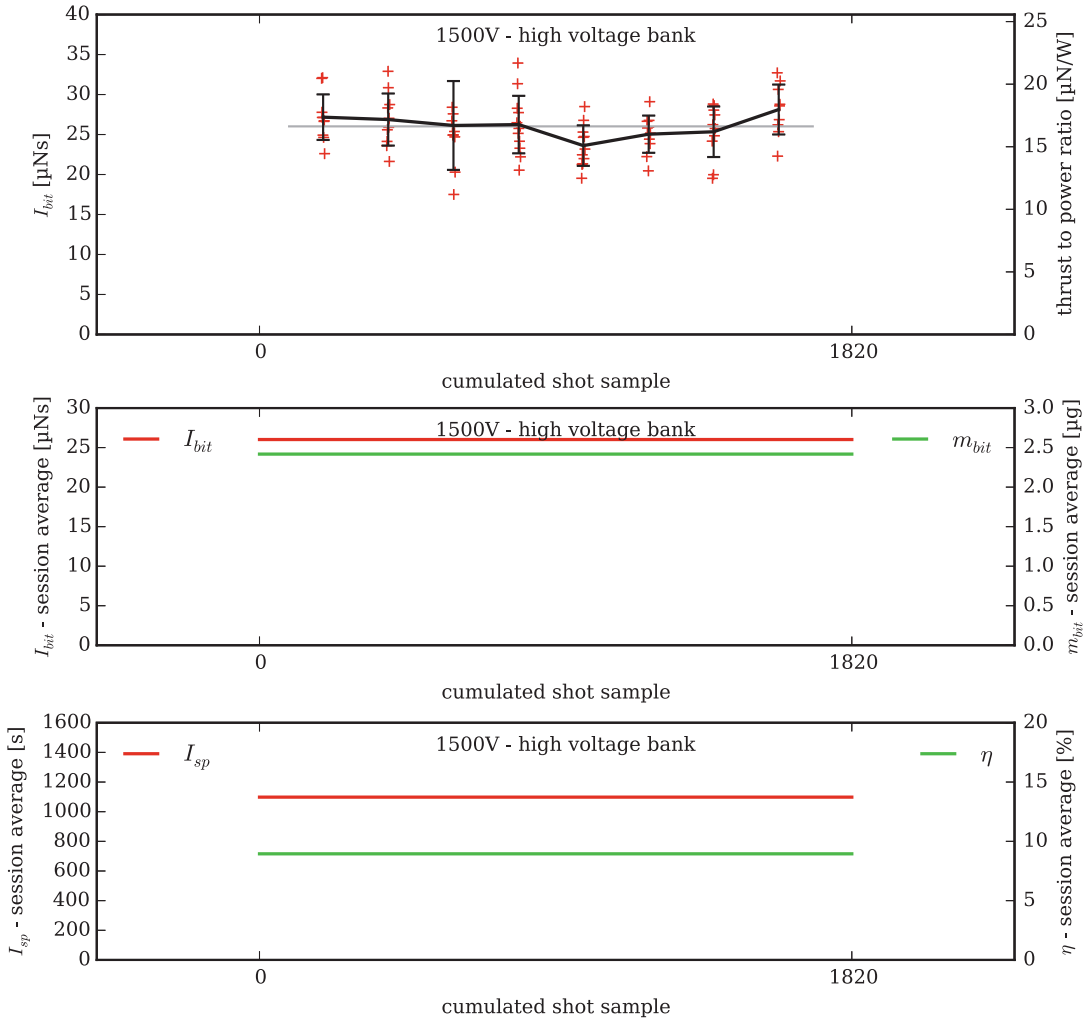

Figure 8. Thruster performance at 1500 V with the high voltage bank (only one experimental session).

E. Performances at 1500 V with the high voltage bank

Due to time constraints, only limited measurements have been made with the high voltage bank, with slightly more than 1800 documented discharges. No issue was noted with this bank during the tests and the bank was still operating nominally at the end of the test. Again, very similar levels of performance in terms of I_{sp} (≈1000 s), thrust-to-power ratio (≈17 µN/W) and efficiency (≈9%) were measured, suggesting that the geometry and general construction of the thruster have more influence on the key performance parameters than the voltage or energy of the capacitor bank.

IV. Discharge characterization

A. Discharge voltage and current measurements

In order to gain preliminary insights on the plasma generation process and its duration, the dynamics of the discharge was monitored with high voltage probes and with two Rogowski coils placed around the anodic copper bridge of each sub-bank, using the low voltage bank characterized at 750 V and 1000 V.

Typical waveforms of the current and voltage are shown on Fig. (9). From an electrical viewpoint, the discharges appear appear very repeatable, and in particular the timing of the maximum of the discharge current is nearly unchanged from discharge to discharge at around 300 ns from triggering.

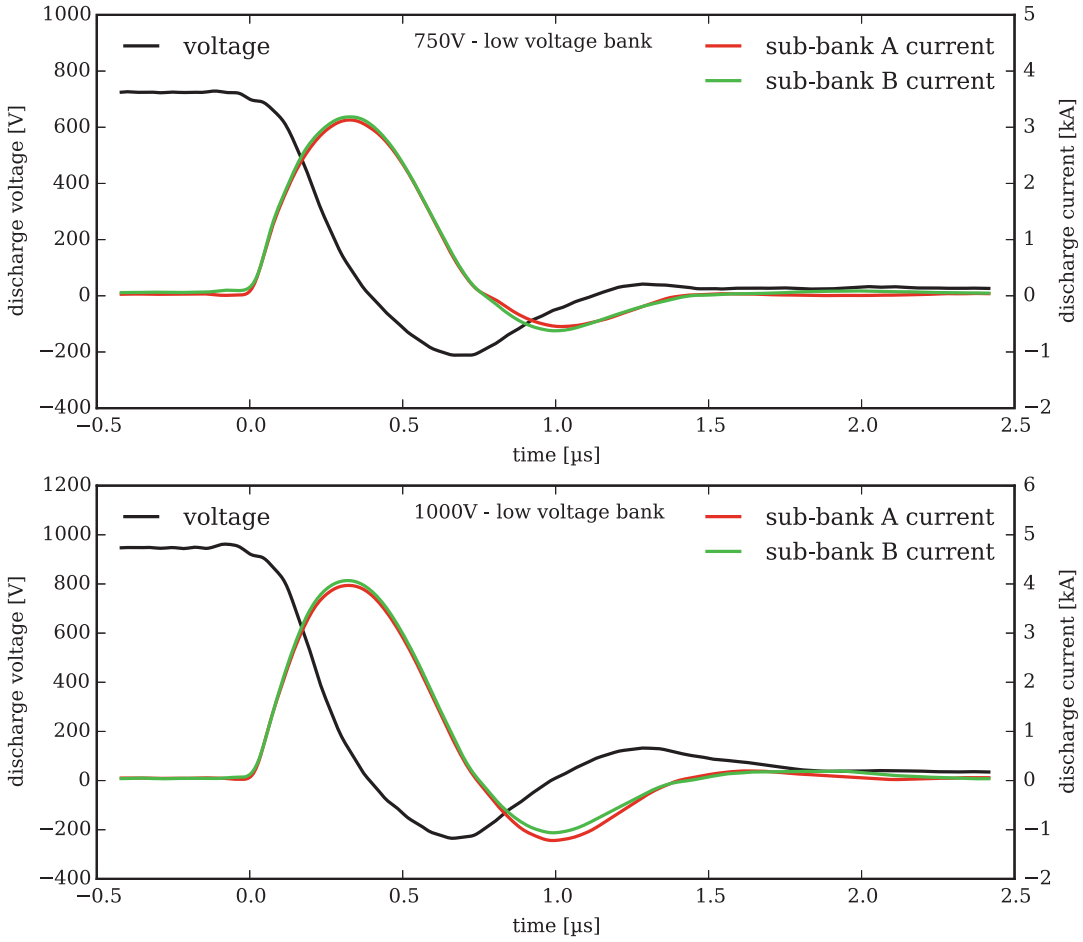

Figure 9. Voltage and current measurements during typical discharges with the low voltage bank. The current is measured individually in each sub-bank with Rogowski coils.

The current in both banks is usually very close, although the discharge does sporadically show some asymmetry which also seems to correlate with an altered visual aspect of the discharge. Some disturbances on the voltage curve are systematically seen just prior to the triggering of the main discharge, which may related to the spark gap ignition.

The current and voltage oscillations show that the discharge is almost critically damped, which for PPTs is usually considered critical to achieve high efficiencies as it allows the energy to be more effectively transferred to the plasma.

Finally, it can be seen that the starting voltage is lower than the specified voltage setting, typically by some 5%, probably because of a miscalibration of the power supply. This implies that the discharge energy used in performance estimates is overestimated and, by consequence, the thrust-to-power ratio and efficiency are somewhat underestimated.

B. Retarded-potential/time-of-flight analysis

Exhaustive retarded potential measurements have been performed at 750 V via a measurement of the current generated by all ions with energies greater than qV_{G2} where q is the charge of the ion species and V_{G2} is the retarding potential applied to the second grid of the RPA.

In order to infer the ion current density at a given retarding potential from the current of all ions with $\epsilon > qV_{G2}$, it is necessary to perform measurements at all desired values of V_{G2} and to subsequently differentiate the collected currents $I_C\,(t,\, V_{G2})$ with respect to V_{G2}. Since the collected signals shows large shot-to-shot variations, however, it is essential to perform many measurements at each single value of V_{G2} and to average such measurements prior to differentiation.

Owing to the very short duration of the L-µPPT discharge in comparison to the time of flight of ions up to the detector (placed in this experiment at 50 cm from the thruster), it is additionally possible to infer the velocity of collected ions from their arrival time. Correlating the velocity and the retarded potential, a combined RPA/time-of-flight analysis makes it possible to discriminate collected ions species, something that is impossible with a standard RPA measurement. Indeed, for an ion species of mass m and charge q, we have:

$$\begin{aligned} V_{G2} &= \frac{1}{2}\frac{m}{q}v^2 \\ &= \frac{1}{2}\frac{m}{q}\frac{L^2}{(t-t_0)^2} \end{aligned}$$

where L is the distance between the thruster and the detector, t is the arrival time and t_0 the time at which ions are assumed to leave the thruster. Each mass-to-charge ratio m/q corresponds to a unique curve in the $(V_{G2},\, t)$ plane and can be identified to a specific type of ion.

The time-of-flight measurement requires, however, a precise estimate of t_0, the time at which ions are created. In order to achieve a precise timing of the beginning of the discharge without immobilizing the thrust balance, a custom non-contact magnetic probe was made and placed near the main electrodes, which measures the electro-motive force generated by the magnetic field created by the discharge. Since the maximum of the discharge current is known to occur at 300 ns after the beginning of the discharge, t_0 was set to 300 ns after the beginning of the pulse recorded by the magnetic probe.

The present results have been derived through the acquisition and averaging of 20 samples at each of the 26 voltages investigated, hence from a total of 520 time-resolved acquisitions. The processed data is plotted on Fig. 10 and is, to the best of our knowledge, the first mass-discriminated analysis of the content of a PPT plasma plume, providing new insights on the underlying physics. Although the correlation with theoretical curves is to some extent subjective, the identification of multiple charge C and F ions appears very compelling.

While this data needs further analysis (in particular at higher potentials), it can already be said that the charge of the ions collected is unexpectedly high. Even though the high visibility of highly charged ions is to some extend due to the fact that the current generated per single particle is proportional to its charge, it appears that the plasma is dominated by F^{3+} and F^{4+}. Due to the closeness of the C^{2+} and C^{3+} charge-to-mass ratio curves with the F^{3+} and F^{5+} ions, it is not possible to conclusively identify them, but C^{4+} ions appear to be present.

These results suggest that the low efficiency of PPTs is to a large extent related to the high production rate of "expensive" —from the energetic viewpoint— ions.

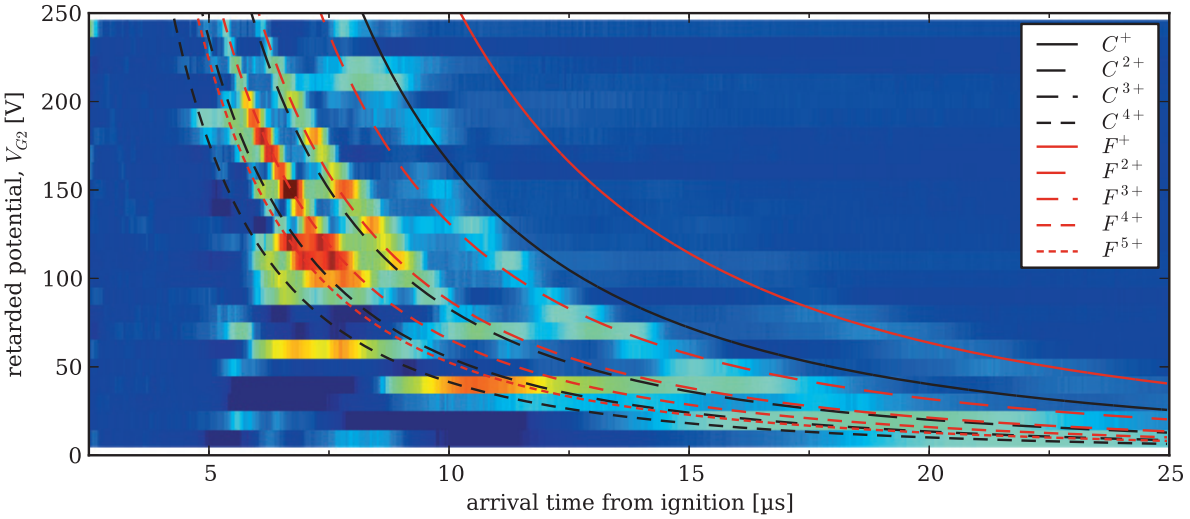

Figure 10. Ion current (color scale) as a function of the retarding potential and time of arrival, shown with the theoretical curves for the m/q ratios of candidate ion species. The data is derived from 520 measurements. Theoretical curves assume $L = 50$ cm, $t_0 = 300$ ns.

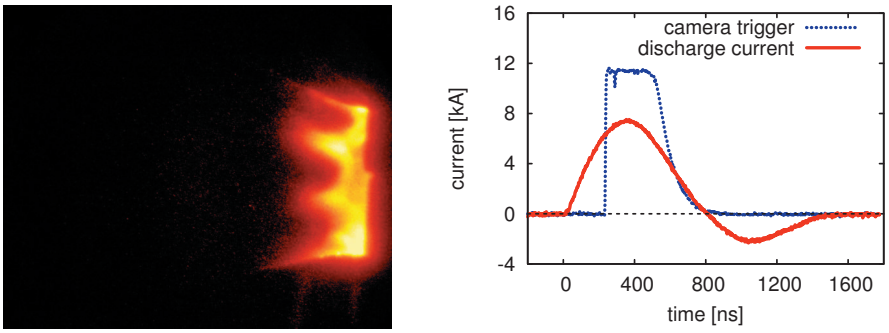

(a) $t = 245\,\mathrm{ns}$

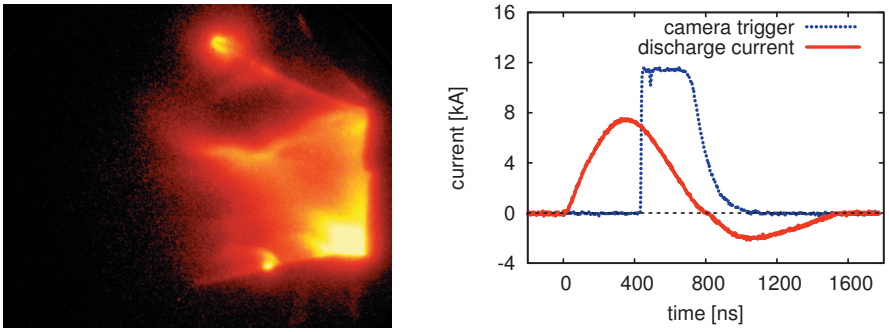

(b) $t = 445\,\mathrm{ns}$

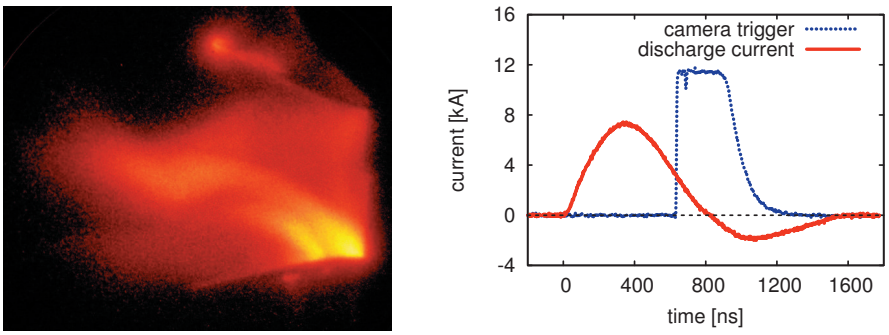

(c) $t = 645\,\mathrm{ns}$

Figure 11. Fast camera frames and corresponding Rogowski current measurements. The blue curve (arbitrary unit) shows the frame acquisition trigger signal.

C. Fast camera imaging of the plasma

A complementary characterization of the discharge was made using ultra-fast camera imaging. For this purpose, a camera manufactured by the ACS company (Warsaw) was used. The camera is a Gated Intensified CCD, single-frame type, with a 350 nm–900 nm spectral band photocathode. All acquisitions were made with a 10 ns exposure time and the camera was triggered via an optic line by the magnetic probe described in section B with a time delay applied by a signal generator.

Although only one frame could be acquired at each discharge, the repeatability of the discharge turned out to be much better than was initially expected from the variability of the impulse bits. Side-by-side comparison of pairs of images acquired from different discharges with the same delay showed in fact very little difference and indicated that a reconstruction of the discharge from single frames was indeed sound. Rogowski coil measurements were made concomitantly and confirmed the good repeatability of the discharge. This is relatively surprising taking into account that RPA measurements showed even more shot-to-shot

variability than impulse bit measurement measurements. One possible explanation is that these variations are associated to fluctuations of the thrust direction, which would be difficult to observe in the small region observed by the fast camera and would have little influence on the current discharge.

Figure 11 shows a small subset of the acquired images, as the full acquisition sequence covers the discharge from ignition up to $t = 1\,\mu$s with 20 different time delays and 2 independent acquisitions per time delay.

While it is difficult to directly interpret these photographs, they are remarkable in that they do not hint at the existence of a propagating current sheet as is usually implicitly assumed when describing the plasma acceleration process in PPTs. Instead, after a rapid initial spatial development of the discharge up to $t \approx 300$ ns, the plasma topology appears to acquire a nearly steady steady-state character from $t \approx 500$ ns with distinct filaments that remain attached to the electrodes up until the end of the discharge, although with a steadily decreasing intensity.

V. Conclusion

A salient point of the performance tests is of course the very high efficiency measured, which proved to be above the state of the art for Teflon PPTs and appeared very stable around 10%, even as the operating voltage or bank capacitance was changed.

Compared to the first prototype, the thrust-to-power ratio has decreased significantly, to the benefit of the specific impulse which was measured above 1000 s in nearly all tests, higher than most PPTs in the low power class. Experience with the first prototype and experimental observations with the second prototype (see section D) have hinted at a relationship between high thrust-to-power ratio and increasing exposed propellant area.

Actual measurements of the bank energy suggest that the thrust-to-power ratio initially estimated for the first prototype[12] was slightly over-estimated and should be revised to some 36 µN/W instead of 44 µN/W, which would still be significant with respect to the state of the art. If high thrust-to-power is preferred to high I_{sp}, it could probably also be achieved with the groove dispenser design used in this work, provided a larger groove width or the use of several parallel dispensing grooves.

Although the lifetime tests have shown that the capacitor reliability remains a critical issue and requires further work, significant improvements have already been made compared to the first prototype.

Carbon deposition over exposed surfaces and electrodes appeared to be similar to that observed in Teflon PPTs. Consistently with our expectations and with the observations made with the first prototype, the dispensing groove remained clean at all times and no charring of the PFPE has ever been observed. This in itself is very significant and confirms the former assertion[12] that PFPE is one of very few polymeric propellant suitable for PPT discharges.

Finally, beyond the innovative technological aspects of this work, unique experimental characterizations of the plasma have been performed with a combined RPA/time-of-flight analysis of the plasma plume and time-resolved fast camera reconstructions of the plasma dynamics.

Acknowledgments

The authors are very indebted to John Rogers of Vishay and to the Vishay development team for their help and voluntary commitment to this project.

The research leading to these results has received funding from the European Community's Seventh Framework Programme (FP7/2007-2013) under grant agreement n°283279 for the L-µPPT project. IPPLM has also received financial support from the Polish fund for science in years 2012-2014 for the execution of a partially funded international project. IPPLM and QuinteScience wish to thank Warsaw-based electronics assembler SEMICON for its dedication and readiness to help with reflow soldering.

References

[1]Ziemer, J. K. and Petr, R. A., "Performance of Gas Fed Pulsed Plasma Thrusters Using Water Vapor Propellant," *Proc. 38th AIAA Joint Propulsion Conference*, No. 2002-4273, American Institute of Aeronautics and Astronautics, Washington, D.C., Indianapolis, 2002.

[2]Scharlemann, C. A., *Investigation of Thrust Mechanism in a Water Fed Pulsed Plasma Thruster*, Ph.D. thesis, Ohio State University, 2003.

[3]Koizumi, H., Kakami, A., Furuta, Y., Komurasaki, K., and Arakawa, Y., "Liquid Propellant Pulsed Plasma Thruster,"

Proc. 28th International Electric Propulsion Conference, No. 2003-87, The Electric Rocket Propulsion Society, Worthington, OH, Toulouse (France), 2003.

[4]Kakami, A., Koizumi, H., Komurasaki, K., and Arakawa, Y., "Design and Performance of Liquid Propellant Pulsed Plasma Thruster," *Vacuum*, Vol. 73, 2004, pp. 419.

[5]Koizumi, H., Komurasaki, K., and Arakawa, Y., "Development of Thrust Stand for low Impulse Measurement from Microthrusters," *Rev. Sci. Instrum.*, Vol. 75, 2004, pp. 3185.

[6]Koizumi, H., Kawazoe, Y., Komurasaki, K., and Arakawa, Y., "Performance Improvement of a Liquid Propellant Pulsed Plasma Thruster," *Proc. 29th International Electric Propulsion Conference*, No. 2005-69, The Electric Rocket Propulsion Society, Worthington, OH, Princeton, NJ, 2005.

[7]Zhu, P., Hou, L. Y., and Zhang, W. Y., "The Effect of Easily Ionized Elements Na and K on the Performance of Pulsed Plasma Thruster using Water Propellant," *Sci Tech China Sci*, Vol. 53, 2010, pp. 2878.

[8]Böhrk, H., Lau, M., Herdrich, G., Hald, H., and Röser, H.-P., "A Porous Flow Control Element for Pulsed Plasma Thrusters," *CEAS Space J.*, 2011, pp. 1.

[9]Masui, S., Okada, T., Kitatomi, M., Kakami, A., and Tachibana, T., "A Pulsed Plasma Thruster Using Dimethyl Ether as Propellant," *Trans. JSASS Aerospace Tech. Japan*, Vol. 10, 2012, pp. 65.

[10]Rezaeiha, A. and Schönherr, T., "Review of Worldwide Activities in Liquid-Fed Pulsed Plasma Thruster," *J. Propul. Power*, Vol. 30, 2014, pp. 253.

[11]Barral, S., Kurzyna, J., Remírez, E., Martin, R., Ortiz, P., Alonso, J., Bottinelli, S., Mabillard, Y., Zaldívar, A., Rangsten, P., and Koppel, C. R., "Development Status of an Open Capillary Pulsed Plasma Thruster with Non-Volatile Liquid Propellant," *Proc. 33rd International Electric Propulsion Conference*, No. 2013-291, The Electric Rocket Propulsion Society, Worthington, OH, Washington, DC, 2013.

[12]Barral, S., Kurzyna, J., Rachubiński, H., Szelecka, A., Remírez, E., Martin, R., Ortiz, P., Alonso, J., Bottinelli, S., Mabillard, Y., Zaldívar, A., Rangsten, P., and Koppel, C. R., "First Experimental Characterization of a Pulsed Plasma Thruster with Non-Volatile Liquid Propellant," *Proc. Space Propulsion 2014*, No. 2980924, Cologne (Germany), 2014.

[13]Haag, T. W., "Thrust Stand for Pulsed Plasma Thrusters," *Rev. Sci. Instrum.*, Vol. 68, 1997, pp. 2060.

[14]Cubbin, E. A., Ziemer, J. K., Choueiri, E. Y., and Jahn, R. G., "Pulsed Thrust Measurements using Laser Interferometry," *Rev. Sci. Instrum.*, Vol. 68, 1997, pp. 2339.

[15]Gamero-Castaño, M., "A Torsional Balance for the Characterization of MicroNewton Thrusters," *Rev. Sci. Instrum.*, Vol. 74, 2003, pp. 4509.

[16]D'Souza, B. C. and Ketsdever, A. D., "Investigation of Time-Dependent Forces on a Nano-Newton-Second Impulse Balance," *Rev. Sci. Instrum.*, Vol. 76, 2005, pp. 015105.

[17]Ketsdever, A. D., D'Souza, B. C., and Lee, R. H., "Thrust Stand Micromass Balance for the Direct Measurement of Specific Impulse," *J. Propul. Power*, Vol. 24, 2008, pp. 1376.

[18]Lilly, T., Pancotti, A., Ketsdever, A., Young, M., and Duncan, J., "Development of a Specific Impulse Balance for a Pulsed Capillary Discharge," *Proc. 44th AIAA Joint Propulsion Conference*, No. 2008-4740, American Institute of Aeronautics and Astronautics, Washington, D.C., Hartford, CT, 2008.

[19]Burton, R. L. and Turchi, P. J., "Pulsed Plasma Thruster," *J. Propul. Power*, Vol. 14, 1998, pp. 716.

[20]Rayburn, C., Campbell, M., Hoskins, W. A., and Cassady, J. R., "Development of a Micro Pulsed Plasma Thruster for the Dawgstar Nanosatellite," *Proc. 36th AIAA Joint Propulsion Conference*, No. 2000-3256, American Institute of Aeronautics and Astronautics, Washington, D.C., Huntsville, AL, 2000.

[21]Guarducci, F., Coletti, M., and Gabriel, S. B., "Design and Testing of a Micro Pulsed Plasma Thruster for Cubesat Application," *Proc. 32nd International Electric Propulsion Conference*, No. 2011-239, The Electric Rocket Propulsion Society, Worthington, OH, Wiesbaden (Germany), 2011.

[22]Cirialli, S., Colleti, M., Guarducci, F., and Gabriel, S. B., "PPTCUP Lifetime Test Results," *Proc. 33rd International Electric Propulsion Conference*, No. 2013-164, The Electric Rocket Propulsion Society, Worthington, OH, Washington, DC, 2013.